

Supplementary Information

White-light emission from the quadruple-stranded dinuclear Eu(III) helicate decorated with pendent tetraphenylethylene (TPE)

Yuying Li, Yanyan Zhou, Yuan Yao, Ting Gao, Pengfei Yan* and Hongfeng Li*

Key Laboratory of Functional Inorganic Material Chemistry, Ministry of Education, P. R. China; School of Chemistry and Materials Science, Heilongjiang University, Harbin 150080, P. R. China.

Synthetic procedures

1,1'-(6,6'-dimethoxy-1,1'-biphenyl-3,3'-diyl)diethanone, 1. A solution of anhydrous aluminium chloride (2.86 g, 21.49 mmol) and acetyl chloride (1.68 g, 21.49 mmol) in dry 1,2-dichloroethane was stirred for 10 min, the mixed solution was slowly dripped into the 1,2-dichloroethane solution of 2,2-dimethoxy-1,1-biphenyl (2.00 g, 9.34 mmol) under the conditions of an ice water bath, after that, stirred for 24 h at rt. The resulting mixture was poured into ice water, the organic layer was dried with anhydrous sodium sulphate, then filtered to remove the salt, the spare solvent was evaporated in vacuo. The crude product was purified by crystallization from ethanol to give white bulk crystals (2.50 g, 89.93 %). ¹H NMR (CDCl₃, 400 MHz) δ 8.01 (m, 2H), 7.85 (d, *J* = 4 Hz, 2H), 7.01 (d, *J* = 8 Hz, 2H), 3.03 (s, 6H), 2.57 (s, 6H). EI-MS *m/z* = 298.12 [M]⁺.

2,2'-Dihydroxy-5,5'-diacetylbiophenyl, 2. A solution of anhydrous aluminium chloride (8.95 g, 67.09 mmol) and **2** (5.00 g, 16.77 mmol) in dry 1,2-dichloroethane was refluxed for 20 min. After cooling the reaction mixture to room temperature, it was filtered. The filtrate was concentrated and the residue was extracted with 5 % NaOH (2 × 120 mL) and washed with water (2 × 60 mL), The resulting white precipitate was filtered and dried in vacuum (3.90 g, 86.09 %). ¹H NMR (CD₃CN 400 MHz) δ 7.91 (m, 2H), 7.16 (d, *J* = 4 Hz, 2H), 7.02 (d, *J* = 8 Hz, 2H), 2.52 (s, 6H). EI-MS *m/z* = 270.08 [M]⁺.

1,1'-(6,6'-di(2-(4-methoxyphenyl)ethene-1,1,2-triyl)tribenzene-1,1'-biphenyl-3,3'-diyl)diethanone, 3. A mixture of **2** (7.00 g, 25.92 mmol) and Cs₂CO₃ (50.67 g, 155.51 mmol) in dry acetone (300 mL) was heated at reflux for 1 h under N₂. Then (2-(4-(bromomethyl)phenyl)ethene-1,1,2-triyl)tribenzene (24.17 g, 57.02 mmol) was added and the mixture was heated at reflux for an additional 1 h. After cooling the reaction mixture to room temperature, it was filtered. The filtrate was concentrated and the residue was extracted with CH₂Cl₂ (2 × 40 mL) and washed with water (2 × 45 mL), dried (Na₂SO₄) and condensed under reduced pressure. The residue was purified by column chromatography on silica gel with Ea/hexane (1:5) as eluent to yield the desired compound **4** as a light yellow solid (17.50 g, 70.56 %). ¹H NMR (CDCl₃, 400 MHz) δ 7.97 (m, 1H), 7.91 (d, *J* = 4 Hz, 1H), 7.03 (m, 33H), 6.91 (m, 5H), 6.80 (d, *J* = 8 Hz, 4H), 4.82 (s, 4H), 2.55 (s, 6H). ESI-MS *m/z* = 981.41 [M + Na]⁺.

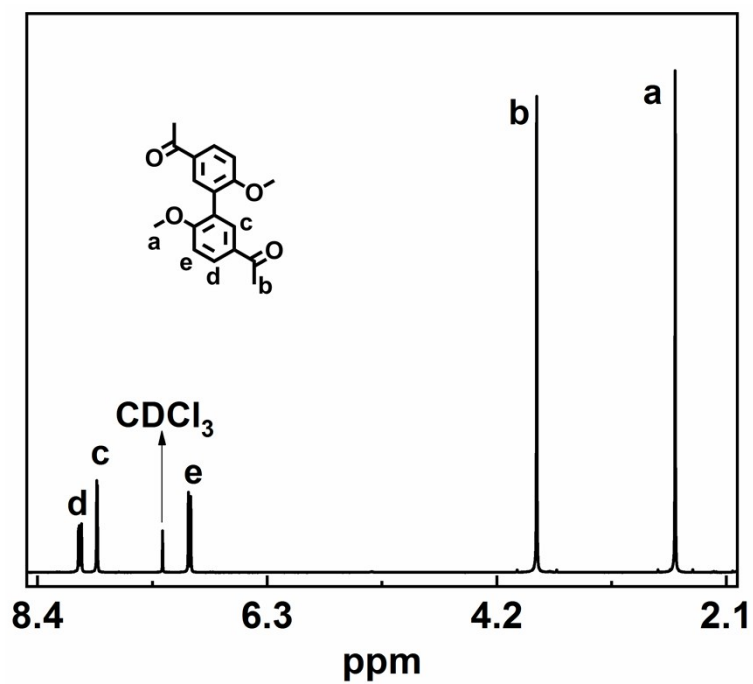


Figure S1. ^1H NMR spectrum of 1 in CDCl_3 .

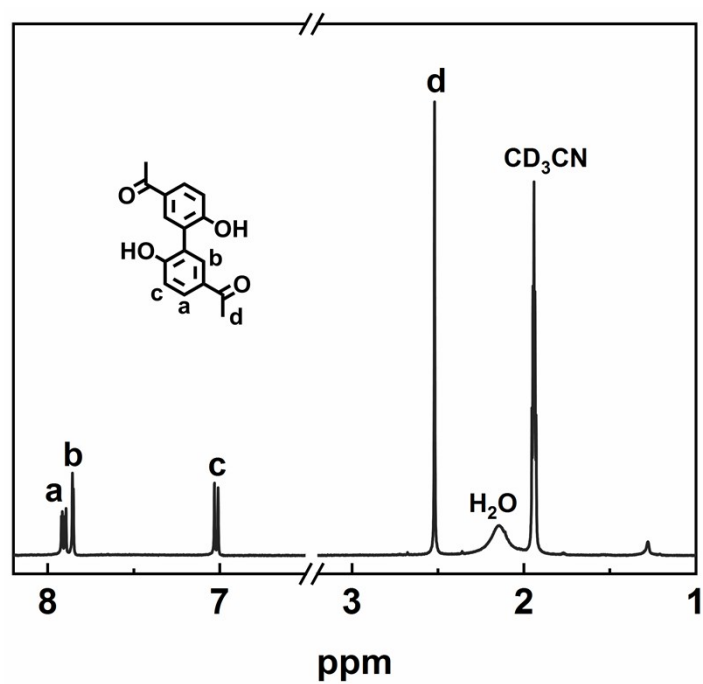


Figure S2. ^1H NMR spectrum of 2 in CD_3CN .

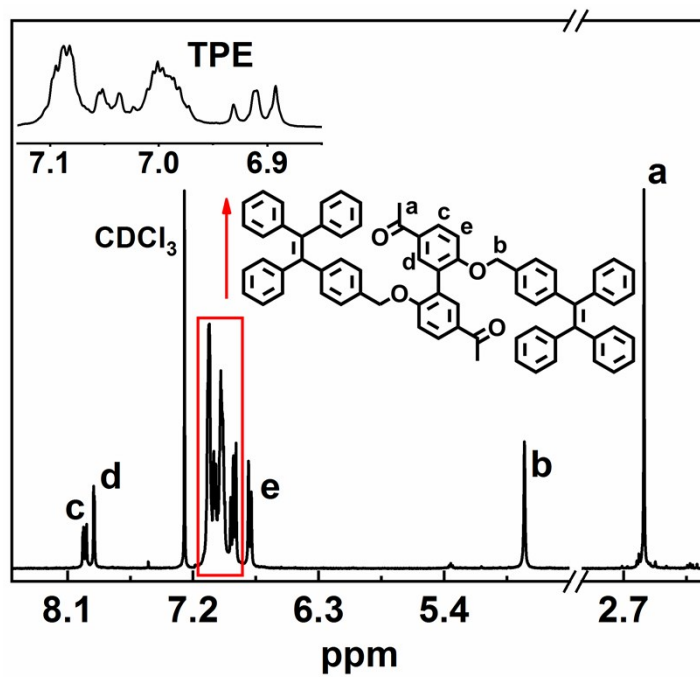


Figure S3. ^1H NMR spectrum of **3** in CDCl_3 .

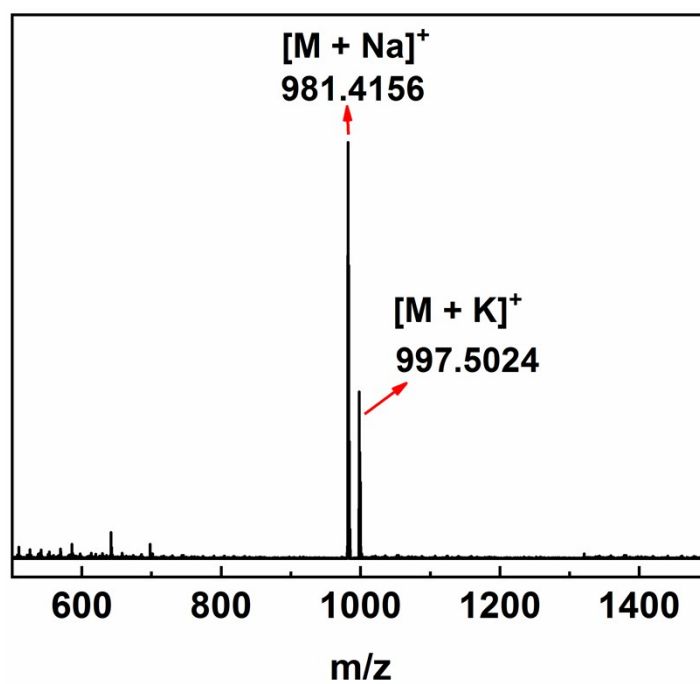


Figure S4. ESI-MS of **3**.

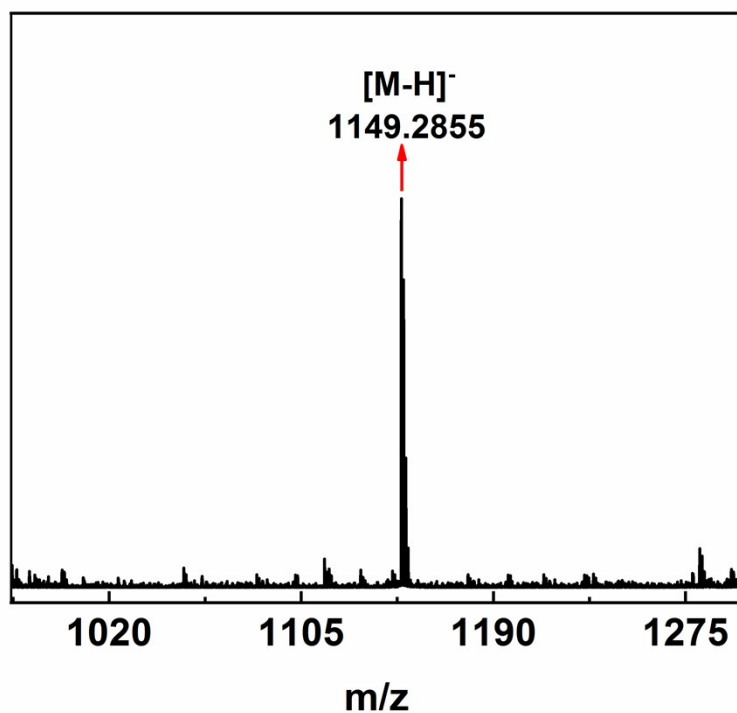


Figure S5. ESI-MS of L¹.

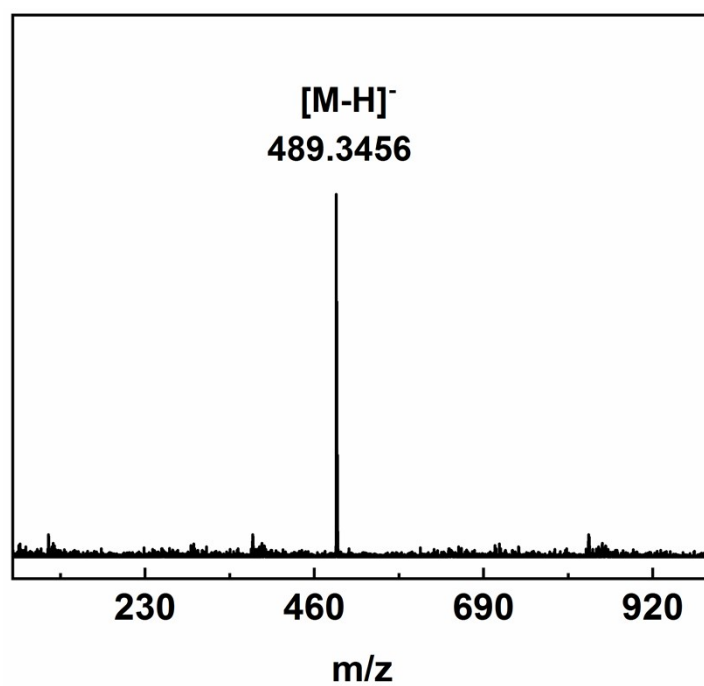


Figure S6. ESI-MS of L².

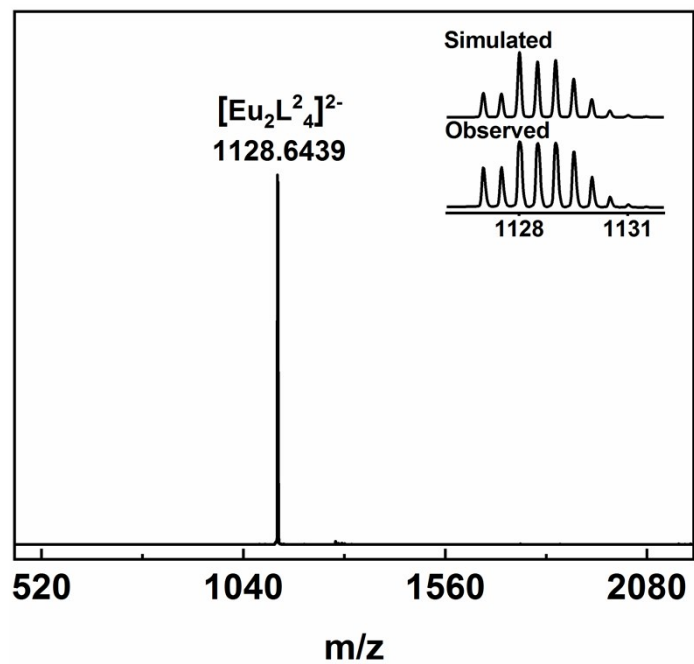


Figure S7. ESI-MS of $(\text{HNEt}_3)_2[\text{Eu}_2\text{L}^2_4]$.

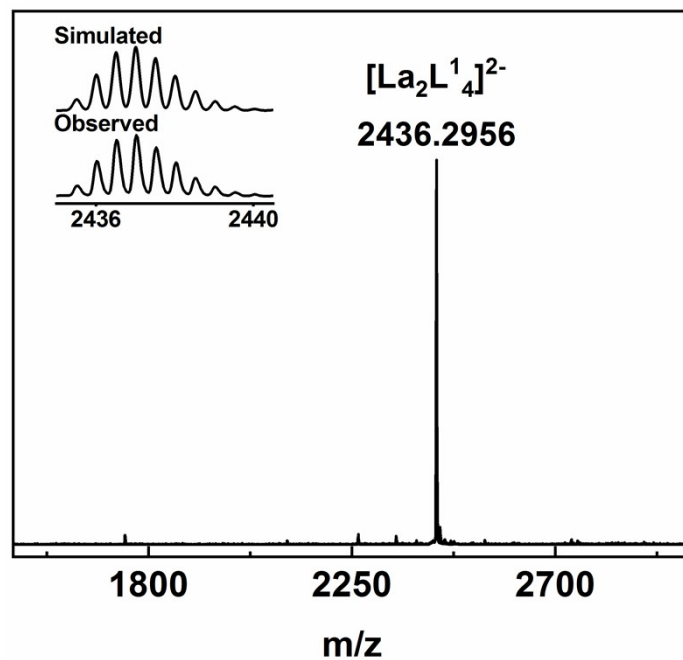


Figure S8. ESI-MS of $(\text{HNEt}_3)_2[\text{La}_2\text{L}^1_4]$.

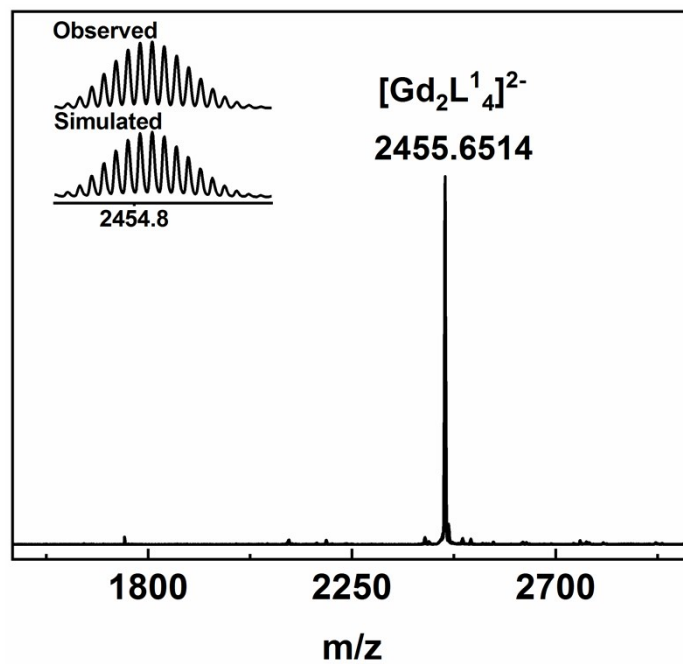


Figure S9. ESI-MS of $(\text{HNEt}_3)_2[\text{Gd}_2\text{L}^1_4]$.

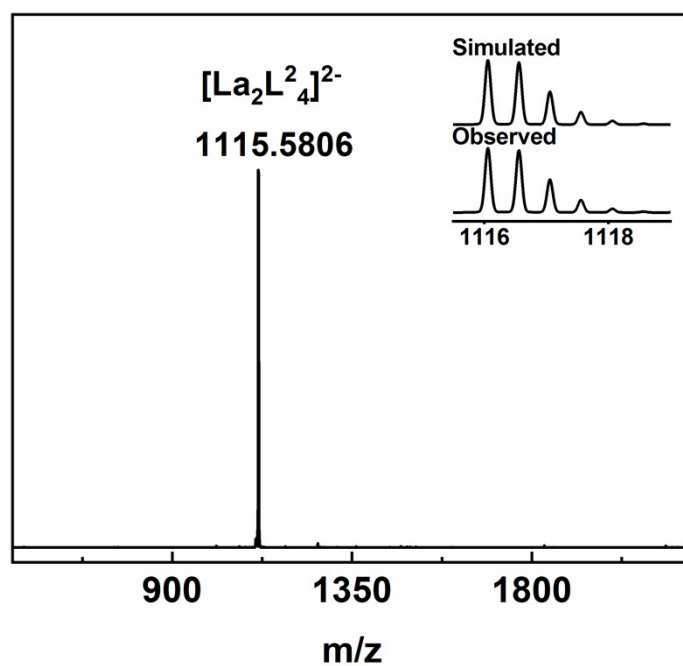


Figure S10. ESI-MS of $(\text{HNEt}_3)_2[\text{La}_2\text{L}^2_4]$.

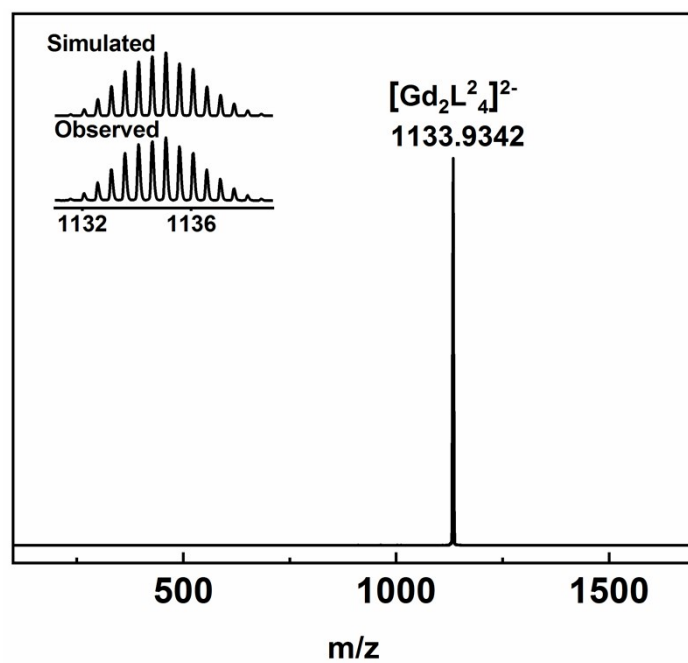


Figure S11. ESI-MS of $(\text{HNEt}_3)_2[\text{Gd}_2\text{L}^2_4]$.

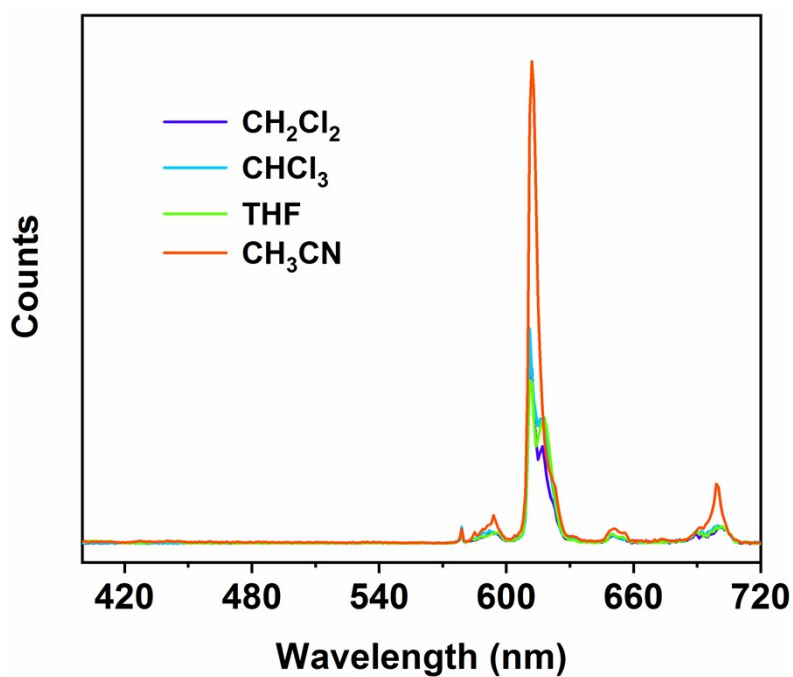


Figure S12. The emission spectra of $(\text{HNEt}_3)_2[\text{Eu}_2\text{L}^1_4]$ in various solvents ($c = 2.5 \times 10^{-6}$ M for complex).

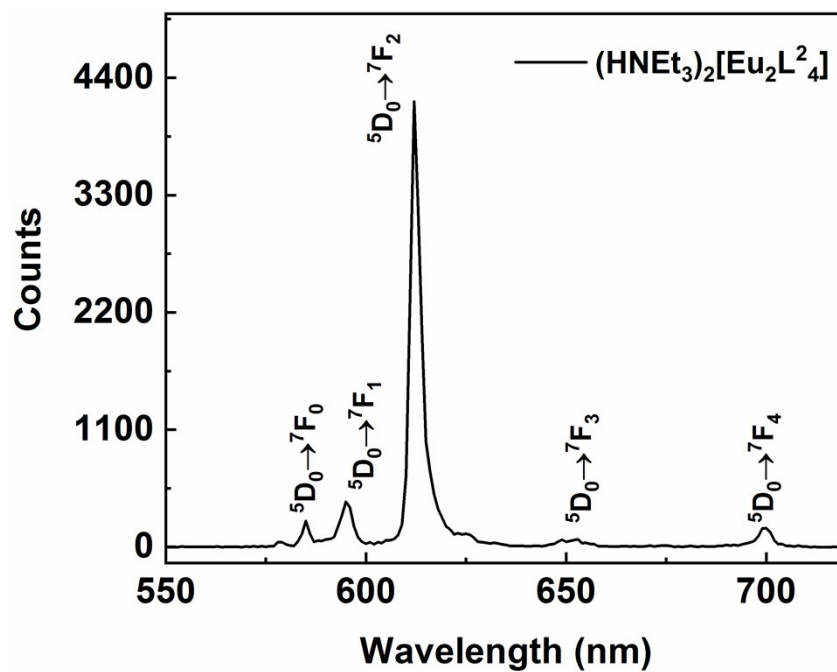


Figure S13. Emission spectrum of the complex $(\text{HNEt}_3)_2[\text{Eu}_2\text{L}^2_4]$ in solid.

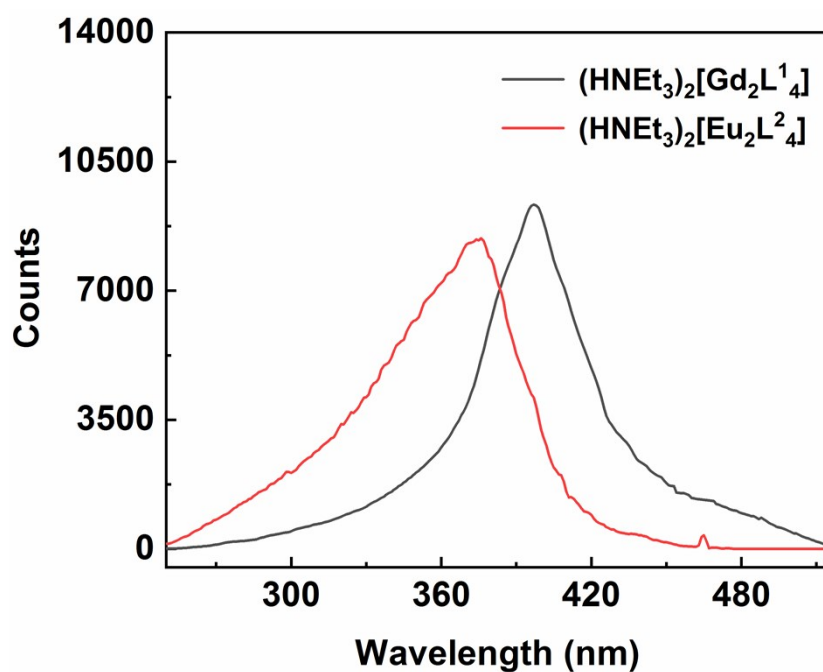


Figure S14. Excitation spectra of $(\text{HNEt}_3)_2[\text{Gd}_2\text{L}^1_4]$ (black line) and $(\text{HNEt}_3)_2[\text{Eu}_2\text{L}^2_4]$ (red line) in solid.

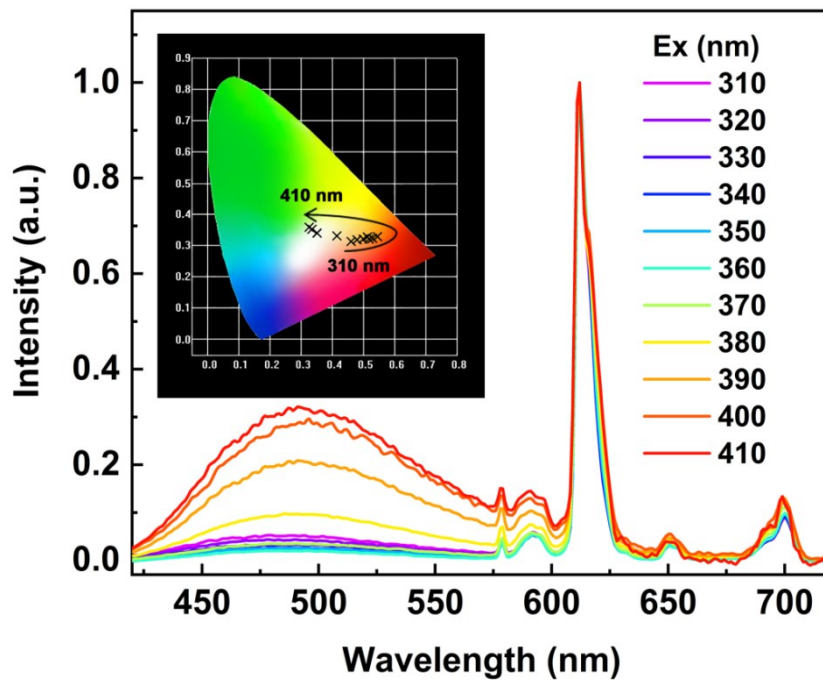


Figure S15. The emission spectra of the films with doping levels of 0.3% with the excitation wavelengths changing from 310 to 410 nm.

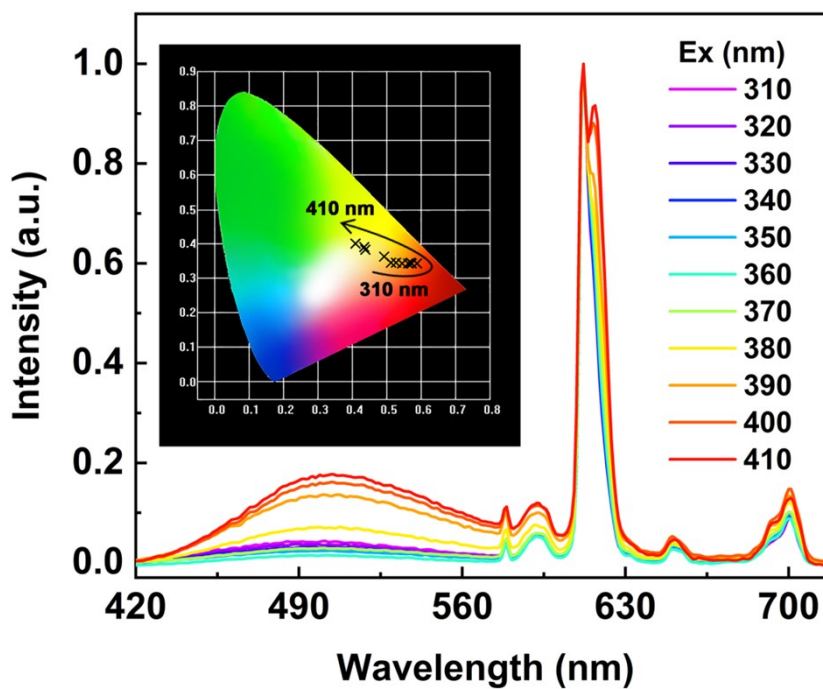


Figure S16. The emission spectra of the films with doping levels of 4% with the excitation wavelengths changing from 310 to 410 nm.

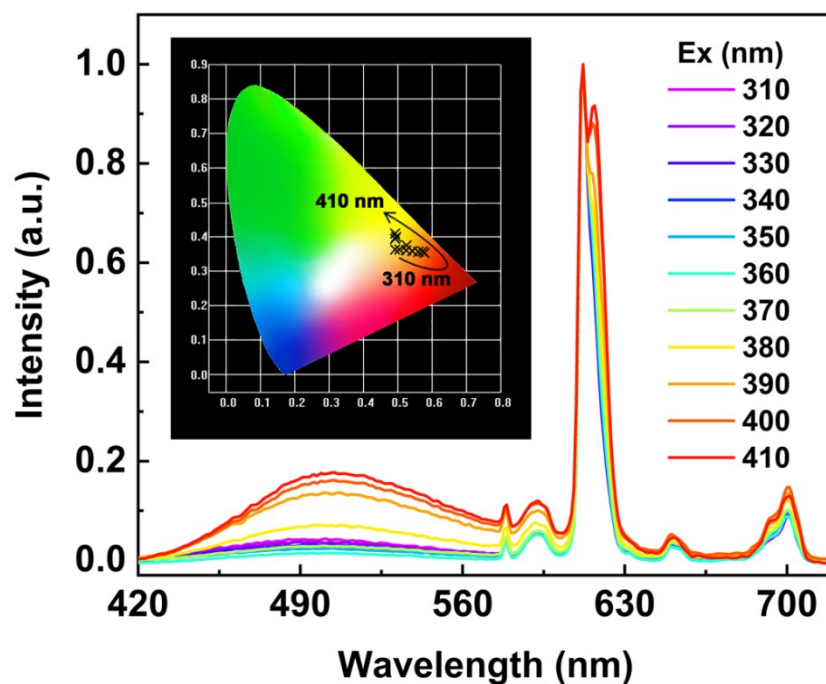


Figure S17. The emission spectra of the films with doping levels of 8% with the excitation wavelengths changing from 310 to 410 nm.

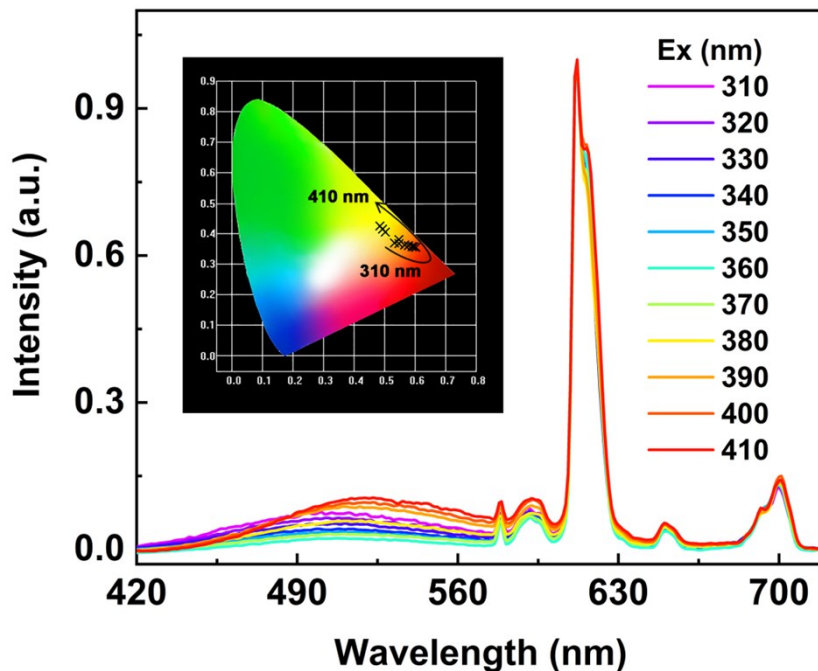


Figure S18. The emission spectra of the films with doping levels of 10% with the excitation wavelengths changing from 310 to 410 nm.

Table S1. Chromaticity coordinates data for the films with doping levels of 0.1, 0.3, 0.5, 2, 4, 8 and 10%.

| Ex (nm) | CIE (x, y) | | | | | | | |
|------------|--------------|--------------|--------------|--------------|--------------|--------------|--------------|--|
| | 0.1% | 0.3% | 0.5% | 2% | 4% | 8% | 10% | |
| 310 | 0.409, 0.302 | 0.460, 0.313 | 0.484, 0.326 | 0.501, 0.330 | 0.512, 0.344 | 0.492, 0.363 | 0.533, 0.370 | |
| 320 | 0.435, 0.310 | 0.480, 0.317 | 0.505, 0.328 | 0.524, 0.333 | 0.528, 0.344 | 0.505, 0.362 | 0.548, 0.367 | |
| 330 | 0.463, 0.313 | 0.500, 0.320 | 0.531, 0.328 | 0.548, 0.333 | 0.546, 0.343 | 0.525, 0.359 | 0.564, 0.363 | |
| 340 | 0.488, 0.316 | 0.517, 0.321 | 0.552, 0.329 | 0.565, 0.333 | 0.563, 0.343 | 0.543, 0.357 | 0.578, 0.359 | |
| 350 | 0.503, 0.318 | 0.530, 0.323 | 0.559, 0.330 | 0.573, 0.333 | 0.572, 0.342 | 0.560, 0.355 | 0.591, 0.357 | |
| 360 | 0.516, 0.322 | 0.544, 0.327 | 0.568, 0.331 | 0.584, 0.335 | 0.587, 0.342 | 0.578, 0.353 | 0.602, 0.355 | |
| 370 | 0.486, 0.323 | 0.513, 0.327 | 0.538, 0.334 | 0.557, 0.338 | 0.569, 0.346 | 0.572, 0.357 | 0.596, 0.358 | |
| 380 | 0.396, 0.324 | 0.414, 0.330 | 0.438, 0.342 | 0.460, 0.350 | 0.493, 0.363 | 0.526, 0.376 | 0.547, 0.380 | |
| 390 | 0.322, 0.332 | 0.349, 0.341 | 0.363, 0.354 | 0.387, 0.362 | 0.437, 0.382 | 0.493, 0.394 | 0.502, 0.404 | |
| 400 | 0.296, 0.329 | 0.334, 0.352 | 0.336, 0.363 | 0.363, 0.372 | 0.434, 0.390 | 0.495, 0.401 | 0.493, 0.414 | |
| 410 | 0.285, 0.299 | 0.324, 0.358 | 0.324, 0.365 | 0.349, 0.380 | 0.430, 0.400 | 0.492, 0.411 | 0.484, 0.425 | |

Table S2. The luminescence quantum yields (QYs) of hybrid films with doping levels of 0.1, 0.3, 0.5, 2, 4, 8 and 10%.

| Doping level (%) | QYs (%) |
|------------------|---------|
| 0.1 | 16.9 |
| 0.3 | 19.5 |
| 0.5 | 13.1 |
| 2 | 12.4 |
| 4 | 12.3 |
| 8 | 8.9 |
| 10 | 6.1 |

Table S3. The color rendering indices (CRIs) and CRI of R9 for the white-emitting films with doping levels of 0.1, 0.3, 0.5, 2, 4, 8 and 10%.

| doping levels (%) | CRI (Ra) | CRI (R9) |
|-------------------|----------|----------|
| 0.1 | 69.37 | 66.16 |
| 0.3 | 63.09 | 55.59 |
| 0.5 | 67.00 | 73.47 |
| 2 | 64.25 | 78.15 |
| 4 | 62.77 | 77.65 |
| 8 | 61.99 | 27.15 |
| 10 | 64.58 | 26.23 |

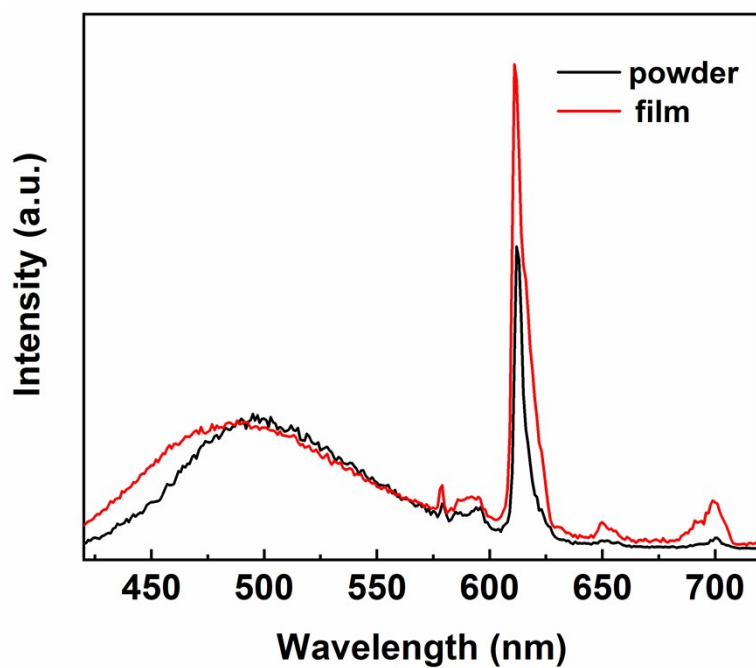


Figure S19. The emission spectra of powder and film with doping level of 0.1%.

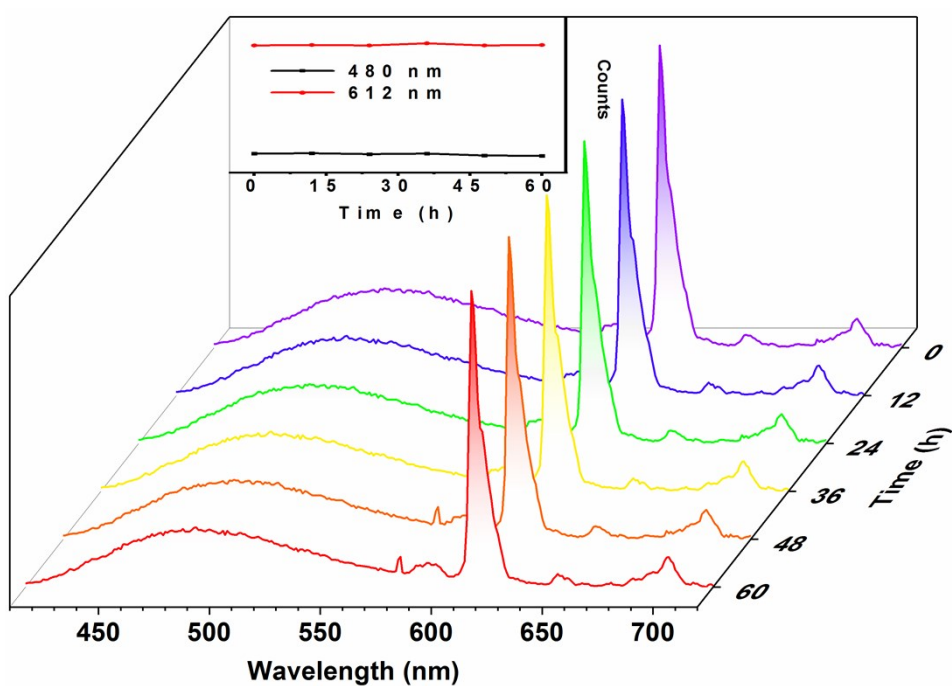


Figure S20. The emission spectra of the film with doping level of 0.1% against the UV excitation of around 390 nm at various hours.

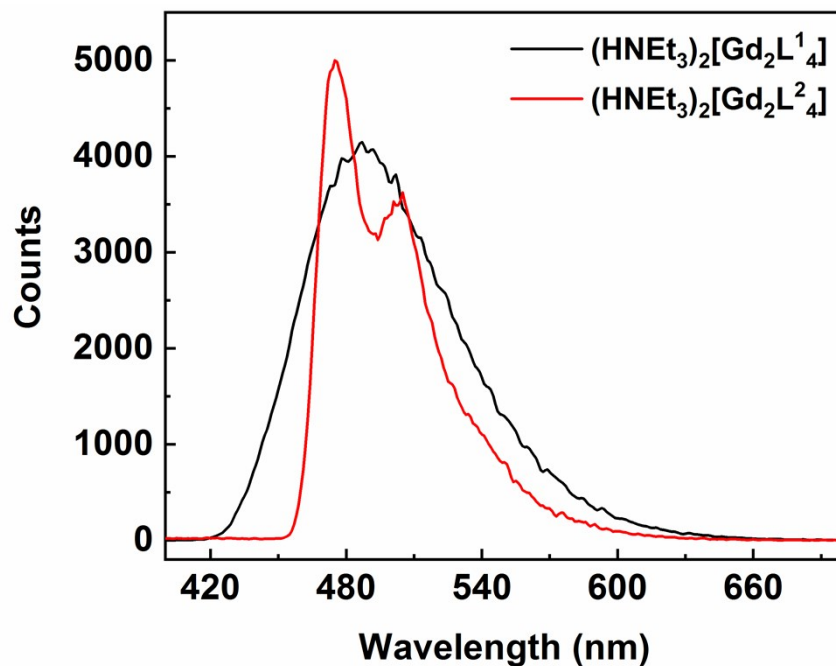


Figure S21. Phosphorescence spectra of $(\text{HNEt}_3)_2[\text{Gd}_2\text{L}^1]$ (black line) and $(\text{HNEt}_3)_2[\text{Gd}_2\text{L}^2]$ (red line) in THF at 77 K.

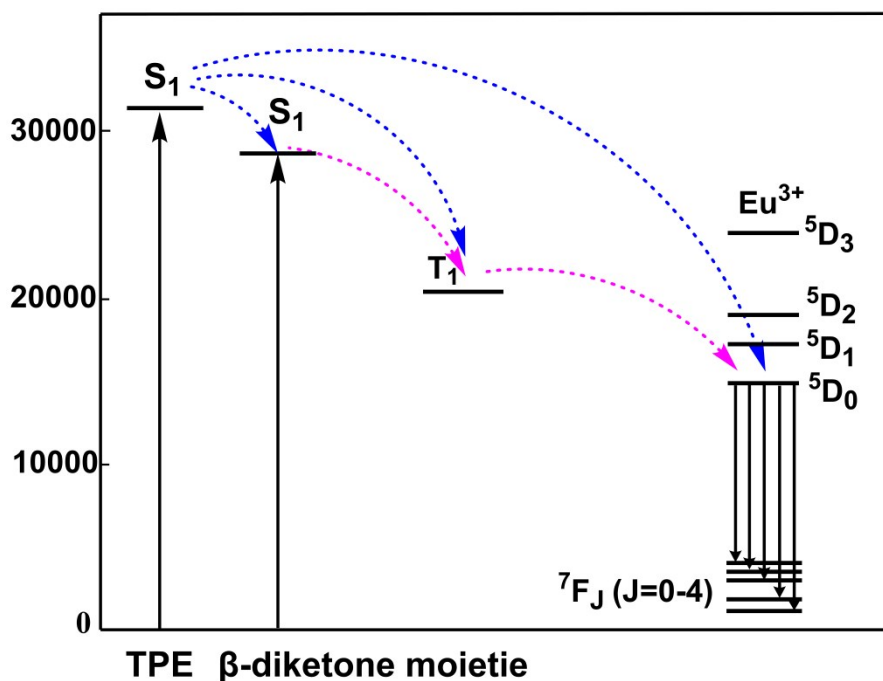


Figure S22. Schematic energy level diagram and energy transfer process for complex $(\text{HNEt}_3)_2[\text{Eu}_2\text{L}^1]$ (S_1 : first excited singlet; T_1 : first excited triplet state).

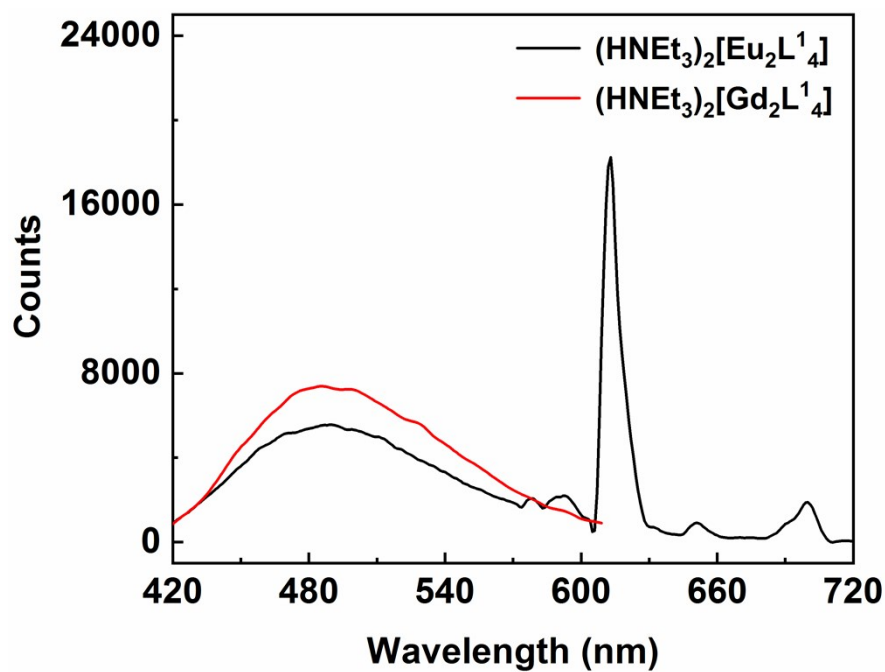


Figure S23. The fluorescence emission of TPE in 0.1% hybrid films of (HNEt₃)₂[Gd₂L¹₄] and (HNEt₃)₂[Eu₂L¹₄]

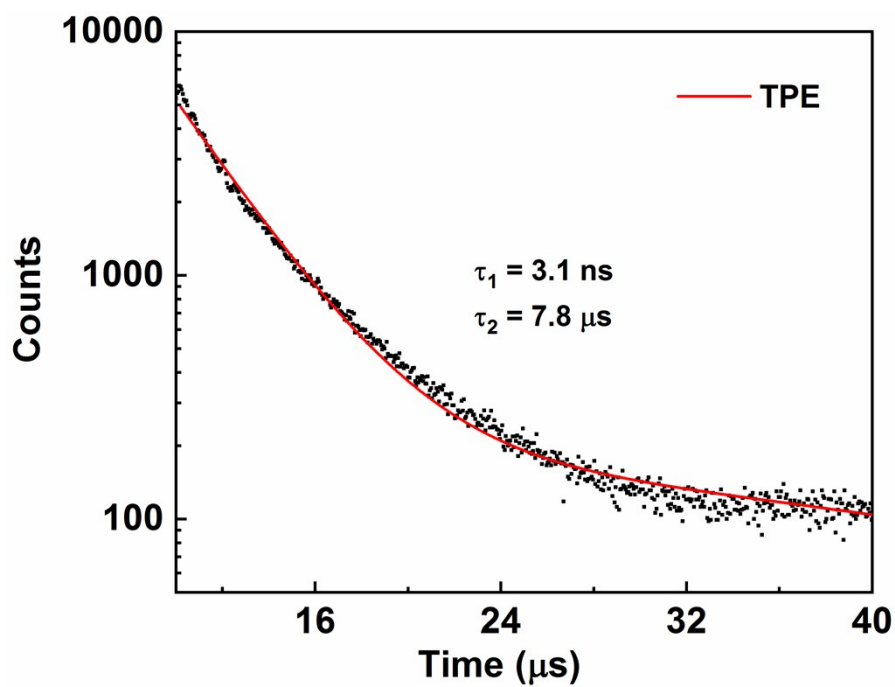


Figure S24. Luminescence decay curve of TPE in 0.1% hybrid film of (HNEt₃)₂[Gd₂L¹₄] at 480 nm.

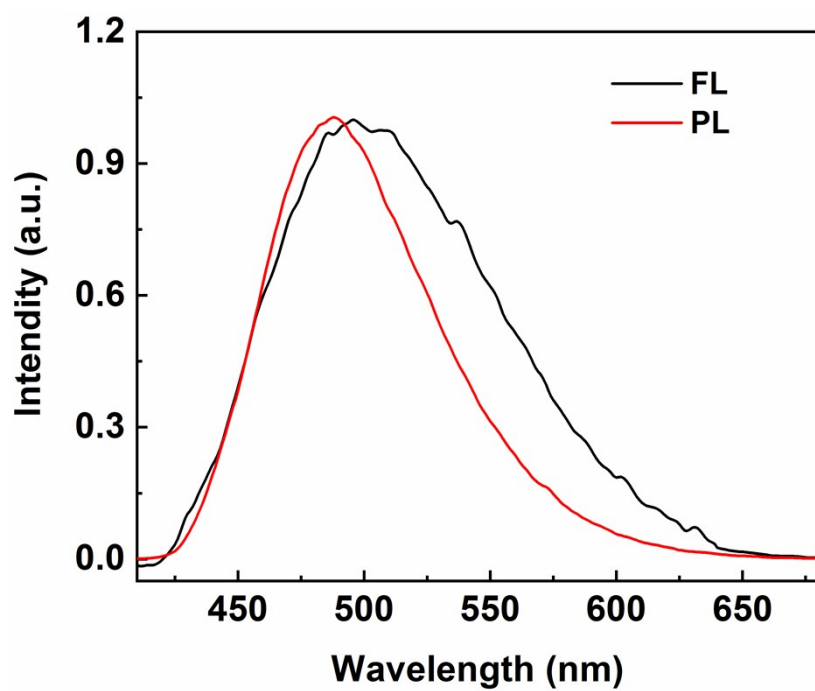


Figure S25. Fluorescence and phosphorescence spectra of $(\text{HNEt}_3)_2[\text{Gd}_2\text{L}_4]$.